

STUDIES ON TRAJECTORY TRACKING OF TWO LINK PLANAR MANIPULATOR

By

Mr. SANE SUBHASH



Department of Mechanical Engineering
National Institute of technology, Rourkela
Rourkela- 769 008, Odisha, INDIA 2012-2014

STUDIES ON TRAJECTORY TRACKING OF TWO LINK PLANAR MANIPULATOR

A Thesis Submitted in Partial Fulfilment of the
Requirements for the Degree of
BACHELOR OF TECHNOLOGY IN MECHANICAL ENGINEERING
AND
MASTER OF TECHNOLOGY IN MECHATRONICS AND AUTOMATION

By
Mr. SANE SUBHASH
710ME4117

Under the supervision of
Prof J SRINIVAS

Department of Mechanical Engineering
National Institute of Technology, Rourkela
MAY, 2015



Department of Mechanical Engineering
National Institute of Technology, Rourkela

CERTIFICATE

This is to certify that the thesis entitled, “STUDIES ON TRAJECTORY TRACKING OF TWO LINK PLANAR MANIPULATOR” by Mr Sane Subhash, submitted to the National Institute of Technology, Rourkela for the award of Master of Technology in Mechanical Engineering with the specialization of “Mechatronics and Automation”, is a record of bonafide research work carried out by him in the Department of Mechanical Engineering, under my supervision and guidance. I believe that this thesis fulfils part of the requirements for the award of the degree of Master of Technology. The results embodied in this thesis have not been submitted for the award of any other degree else other.

Dr. (Prof.) J. Srinivas

Dept. of Mechanical Engineering

National Institute of Technology

Rourkela-769008,

Odisha, INDIA

Place:

Date :

ACKNOWLEDGEMENT

First and foremost, I wish to express my sense of gratitude and indebtedness to my supervisor Prof. J. Srinivas for their inspiring guidance, encouragement, and untiring efforts throughout the course of this work. Their timely help, constructive criticism and painstaking efforts made it possible to present the work contained in this thesis.

I express my gratitude to the professors of my specializations for their advice and care during my tenure. I am also very much obliged to the Head of Department of Mechanical Engineering Prof. S S Mohapatra NIT Rourkela for providing all the possible facilities towards this work. Also thanks to the other faculty members in the department.

Specially, I extend my deep sense of indebtedness and gratitude to my colleagues, Mr Satish, Teja and Madhusmita and my senior, Ms. Varlakshmi madam for their helpful company. After the completion of this Thesis, I experience a feeling of achievement and satisfaction. Looking into the past I realize how impossible it was for me to succeed on my own. I wish to express my deep gratitude to all those who extended their helping hands towards me in various ways during my tenure at NIT Rourkela

ABSTRACT

In robotic manipulator control situations, high accuracy trajectory tracking is one of the challenging aspects. This is due to nonlinearities in dynamics and input coupling present in the robotic arm. In the present work, a two link planar manipulator revolving in a horizontal plane is considered. Its kinematics, Jacobian analysis, dynamic equations are obtained from modelling. It is proposed to use this manipulator for following a desired trajectory by using an effective control method. Initially, computed torque control scheme is used to obtain the end effector motions. The dynamic equations are solved by numerical method and the joint space results are used to obtain the error and its derivative. This linearized error dynamic control uses constant gains and an attempt is made to obtain a correct set of gains in each error cycle to refine the control performance. A scaled prototype is made with aluminium links and joint servos. A mechatronic system with an arduino microcontroller board is employed to drive the servos in incremental fashion as per the tracking point and its inverse kinematics. The computer results are shown for two trajectories namely a straight line and spline. The errors are reported as a function of time and the corresponding joint torques computed in each time step are plotted. Finally to illustrate the mechatronic control system on the prototype, a path containing three points is considered and corresponding errors and repeatability are presented.

INDEX

List of Figures.....vii

List of Tables.....viii

Chapter 1

Introduction.....	1
1.1. Manipulator Analysis and Control.....	2
1.2. Literature Review on Two Link Serial Manipulator.....	3
1.3. Objectives of the present work.....	3

Chapter 2

Mathematical Modelling.....	5
2.1. Kinematic Analysis.....	5
2.2. Inverse Kinematics.....	7
2.3. Jacobian.....	7
2.4. Dynamics.....	9
2.5. Solution of Dynamic Equation.....	10
2.6. Computed Torque Control Method.....	10

Chapter 3

Results and Discussion.....	12
3.1. Workspace Analysis.....	12
3.2. Manipulability Index.....	13
3.3. Static Force Analysis.....	13
3.4. Inverse Dynamic Analysis.....	15
3.5. Control Results.....	16
3.6. Model Fabrication and testing.....	21

Chapter 4

Conclusion.....	24
4.1. Future Scope.....	24

References.....25

Appendix 1.....26

Appendix 2.....27

List of Figures

Fig.1: SCARA Selective Compliance Assembly Robot Arm

Fig.2: Schematic representation of two-link manipulator.

Fig.3: CTC control scheme

Fig.4: Workspace

Fig.5: Manipulability index

Fig.6: Joint torque T_1

Fig.7: Joint torque T_1

Fig.8: Joint torques

Fig.9: Desired trajectory

Fig.10: Trajectory tracking of end effector

Fig.11: Joint angle

Fig.12: Joint velocities

Fig.13: Control torques

Fig.14: Tracking errors

Fig.15: Desired trajectory

Fig.16: Trajectory tracking of end effector

Fig.17: Control torques

Fig.18: Tracking errors

Fig.19: Prototype model

Fig.20: Control experiment for tracking points

Fig.21: Experimental plots for inverse kinematics

List of Tables

Table 1: D-H parameters of two-link manipulator

Table 2: Two-link arm geometric parameters

Table 3: Inverse kinematics solutions

Table 4: Trajectory tracking for inverse kinematics

Chapter 1

INTRODUCTION

A robot's manipulator arm can move within three axes of x , y and z referring to base part, vertical elevation and horizontal extension. Many manipulator types are available as rectangular, cylindrical, spherical, revolute and articulated robotic arm are generally used in industries. Final goal of those robotic designs is to accurate tip position control in spite of the flexibility in a reasonable amount of time. Many controller algorithms those are, adaptive control, Neural Network (NN), fuzzy logic have been used for tip position control of two-link flexible manipulators. These three methods are very effective but are more complex and difficult to design and analyse. So a simple PD controller is implemented on the dynamic model of the flexible manipulator. The proportional-derivative (PD) controllers are more helpful in industry for many years due to their simplicity of operation, robustness of performance. Unfortunately, it has been a problem to achieve optimal PD gains because many industrial plants are often burdened with problems such as high order, time delays, and nonlinearities. The tuning process need labour and time consuming. Due to these reasons, it is highly desirable to find new approaches to the tuning of PD controllers. In this thesis a new PD controller design is done via root locus based loop shaping approach. In many field applications where technical support is required, man-handling is either dangerous or is not possible. In such situations three or more arm manipulators are commonly used. Some robots are used to inspect dangerous areas or/and to remove and to destroy explosive devices. These robots can be used to make some corridors through mined battle fields, manipulation and neutralization of the intact ammunition, inspection of the vehicles, trains, airplanes and buildings. For these robots a good functional activity is to determinate the dimensions of the workspace, kinematics and control strategies of the robotic arm. Last two decades, conception and use of robots has evolved from the stuff of science fiction films to the reality of computer-controlled electromechanical devices integrated into a wide variety of industrial environments. It is routine to see robot manipulators being used for welding and painting car bodies on assembly lines, stuffing printed circuit boards with IC components, inspecting and repairing structures in nuclear, undersea, and underground environments. Although few of these manipulators are anthropomorphic, our fascination with humanoid machines has not dulled, and people still envision robots as evolving into electromechanical replicas of ourselves.

1.1. Manipulator Analysis and Control

A manipulator is a mechanical device which can operate remote objects or material even in the absence of any worker. Links and joints make a long chain in a manipulator, which can manipulate in its workspace. The total number of joints gives the degrees-of-freedom (DOF). Manipulators are classified into two types namely:

- 1) Parallel manipulators
- 2) Serial manipulators

Most industrial robots are the serial manipulators which are designed as series of links connected by motor actuated joints from base part to end effector part. These type of manipulators have an anthropomorphic arm structure with a shoulder, an elbow, and a wrist. The main application for these serial type manipulators in present industry is pick and place assembly robot. SCARA is one example for this type of robot and is shown in Fig.1. In this part of work some exceptional control methods for the following control of robot controllers are discussed. The controllers that are created in this part address computational issues and the impacts of actuator motion.

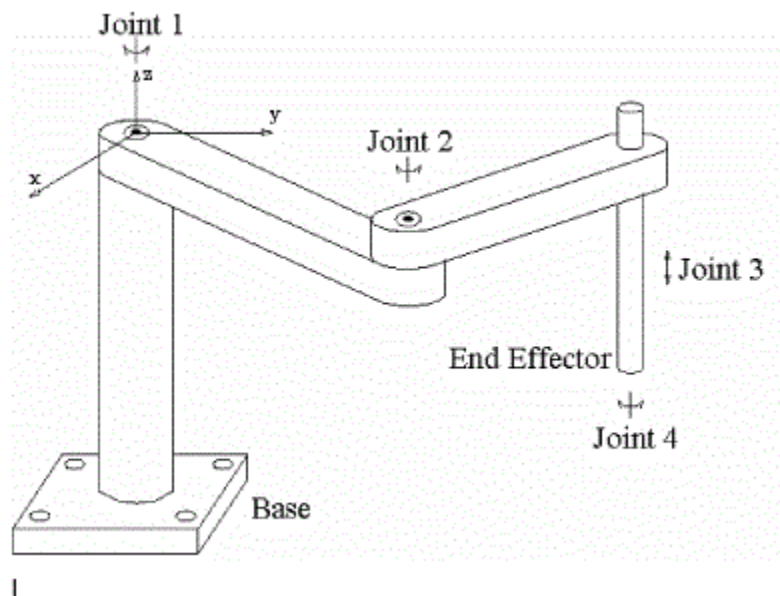


Figure 1: SCARA Selective Compliance Assembly Robot Arm

1.2. Literature Review

Literature survey was conducted to obtain some insights into various factors relating to modelling of planar manipulators for various industrial applications. In this work several aspects regarding the kinematics, workspace, Jacobian analysis and dynamic identification of a two-link planar manipulator are studied and presented. De Luca and Siciliano [1] presented the kinematic and dynamic issues of planar link manipulator. William [2] described automatic Control Systems, analysis and design of serial manipulators. Kwanho [3] explained the adaptive control of tip point in a serial link robot. Nagrath and Gopal [4] explained various issues like kinematics, dynamics, control theories for different serial manipulators. Tokhi and Azad [5] discussed the kinematic and modelling of flexible manipulators. Finally the proposed control method is applied for the flexible manipulator to illustrate the results. Ata [6] presented the review on various optimal trajectory planning control techniques for serial manipulators. Islam and Liu [7] proposed a sliding mode control technique to serial manipulator and studied the. Kumara et al. [8] explained trajectory tracking control of kinematically redundant robot manipulators using neural network. Moldoveanu et al. [9] explained a trajectory control of a two-link robot manipulator using variable structure theory. Wang and Deng et al. [10] explained the design of articulated inspection arm with an embedded camera and interchangeable tools. Zhu et al. [11] presented the structure of a serial link robot with 8 degrees of freedom with a 3-axes wrist carrying camera. Ionescu [12] described an approach of measurement using a calibrated Cr252 neutron source deployed by in-vessel remote handling boom and mascot manipulator for JOET vacuum vessel. Monochrome CCD cameras were used as image sensors. Karagulle and Malgaca [13] proposed the effect of flexibility on the trajectory of a planar two-link manipulator is studied using integrated computer-aided design procedures. Nagesh Rao et al. [14] explained the passivity based control method. Detailed algorithm was proposed and implemented for 2-DOF manipulator. Ayala and Coelho [15] illustrated an algorithm to test the PID tuning by using a two degree of freedom robot manipulator.

1.3. Objectives of the present work

In present work, the main objectives to be carried out are kinematic analysis, inverse kinematic analysis, Jacobian analysis, dynamics and solution of dynamic equations. In the part of results and discussions following things are presented: workspace analysis,

manipulability index, static force analysis, inverse dynamic analysis, control results and model fabrication and control. For workspace analysis, a C program based on forward kinematic equations is used. An Arduino program is used to control two servo motors for tracking the given points within the workspace. A Computed Torque Control scheme is used to obtain the trajectory and a task space set point control approach is also presented.

The thesis is organised as follows: Chapter 2 describes mathematical modelling, where the details of two link manipulator including dynamics are presented. Also control algorithm based on CTC is given.

Chapter 3 describes the results and discussion as program outputs and experimentally analysis outcomes.

Chapter 4 gives the brief conclusion.

Chapter 2

Mathematical Modelling

2.1. Kinematic Analysis

Modelling of two-link planar manipulator involves the linear and rotational dynamics of the links. For simplicity it is assumed that the two-link manipulator has two revolute joints and is an open kinematic chain type. Fig. 2 shows the schematic diagram of the two-link manipulator. Let L_1 and L_2 be the length of the first and second link respectively. Angle θ_1 and θ_2 represent the joint rotations of the first, and second joint respectively.

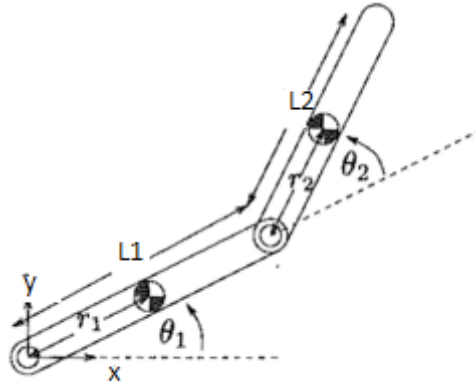


Figure 2: Schematic representation of two-link manipulator

Calculating the position and orientation of the end-effector in terms of the joint variables is called as forward kinematics. In order to have forward kinematics for a robot mechanism in a systematic manner, one should use a suitable kinematics model. Denavit-Hartenberg method that uses four parameters is the most common method for describing the robot kinematics. The parameters of two-link planar manipulator is shown in Table 1. Generalized form of homogenous transformation matrix can be expressed as in equation (1).

$$T_i^{i+1} = \begin{bmatrix} \cos \theta_i & -\sin \theta_i \cos \alpha_i & \sin \theta_i \sin \alpha_i & a_i \cos \theta_i \\ \sin \theta_i & \cos \theta_i \cos \alpha_i & -\cos \theta_i \sin \alpha_i & a_i \sin \theta_i \\ 0 & \sin \alpha_i & \cos \alpha_i & d_i \\ 0 & 0 & 0 & 1 \end{bmatrix} \quad (1)$$

Here, θ_i is joint angle, α_i is link twist a_i is link length and d_i is joint distance

From the D-H parameters shown in Table 1 the overall transformation matrix was derived as:

$$T_2^0 = T_1^0 T_2^1 \quad (2)$$

Table 1: D-H parameters of two-link manipulator

Link	a_i	α_i	d_i	θ_i
1	L_1	0	0	θ_1
2	L_2	0	0	θ_2

Using,

$$C_1 = \cos(\theta_1) \quad S_1 = \sin(\theta_1) \quad S_2 = \sin(\theta_2) \quad C_2 = \cos(\theta_2)$$

For First Link:

$$T_1^0 = \begin{bmatrix} C_1 & -S_1 & 0 & L_1 C_1 \\ S_1 & C_1 & 0 & L_1 S_1 \\ 0 & 0 & 1 & 0 \\ 0 & 0 & 0 & 1 \end{bmatrix} \quad (3)$$

For Second Link:

$$T_2^1 = \begin{bmatrix} C_2 & -S_2 & 0 & L_2 C_2 \\ S_2 & C_2 & 0 & L_2 S_2 \\ 0 & 0 & 1 & 0 \\ 0 & 0 & 0 & 1 \end{bmatrix} \quad (4)$$

By substituting equations (2) and (3) in (1)

The overall manipulator transformation matrix is

$$T_2^0 = \begin{bmatrix} C_{12} & -S_{12} & 0 & L_1 C_1 + L_2 C_{12} \\ S_{12} & C_{12} & 0 & L_1 S_1 + L_2 S_{12} \\ 0 & 0 & 1 & 0 \\ 0 & 0 & 0 & 1 \end{bmatrix} \quad (5)$$

For a 2 DOF planar manipulator P_x, P_y as task coordinates the forward kinematic equations obtained as the last column elements as follows:

$$P_x = L_1 \cos \theta_1 + L_2 \cos(\theta_1 + \theta_2) \quad (6)$$

$$P_y = L_1 \sin \theta_1 + L_2 \sin(\theta_1 + \theta_2) \quad (7)$$

2.2. Inverse Kinematics

Solving the inverse kinematics is computationally expensive and generally takes a very long time in the real time control of manipulators. Tasks to be performed by a manipulator are in the Cartesian space, whereas actuators work in joint space. Cartesian space includes orientation matrix and position vector. However, joint space is represented by joint angles. The conversion of the position and orientation of a manipulator end-effector from Cartesian space to joint space is called as inverse kinematics problem. There are two solutions approaches namely, geometric and algebraic used for deriving the inverse kinematics solution, analytically. The following equations are obtained by algebraic method.

$$\theta_2 = \pm a \tan \frac{\sin \theta_2}{\cos \theta_2} \quad (8)$$

Where,

$$\cos(\theta_2) = \frac{1}{2L_1L_2} (P_x^2 + P_y^2 - L_1^2 - L_2^2) \quad (9)$$

$$\sin(\theta_2) = \pm \sqrt{1 - \cos^2 \theta_2} \quad (10)$$

$$\theta_1 = \text{atan} \frac{S_2}{C_2} \quad (11)$$

Where,

$$S_1 = \frac{(L_1 + L_2 C_2)P_y - L_2 S_2 P_x}{L_1^2 + L_2^2 + 2L_1 L_2 C_2} \quad (12)$$

$$C_1 = \frac{P_x + L_2 S_1 S_2}{L_1 + L_2 C_2}$$

2.3. Jacobian Analysis

In trajectory tracking control it is not just enough to determine the joint and end effector coordinates. It is necessary to control the velocity of the end effector or the tool during the motion. Since the control action occurs at the joints, it is only possible to control the joint velocities. Therefore, there is a need to be able to take the desired end effector

velocities and calculate from them the joint velocities. Since we control the robot in joint space and have a tendency to reason about movement in Cartesian space, we need to completely comprehend the mapping from joint space to Cartesian space and the other way around. Forward and inverse kinematics describes the static relationship between these spaces.

The matrix which relates changes in joint parameter velocities to Cartesian velocities is called the Jacobian Matrix. This is a time-varying, position dependent linear transform. It has a number of columns equal to the number of degrees of freedom in joint space, and a number of rows equal to the number of degrees of freedom in Cartesian space. The Jacobian for this manipulator is:

The matrix which relates changes in joint parameter speeds to Cartesian speeds is known as the Jacobian Matrix. It depends on time-varying, position dependent linear transform. It has various sections equivalent to the quantity of degrees of freedom in joint space, and number of rows equivalent to the degrees of freedom in Cartesian space. The Jacobian for this planar manipulator is:

By differentiating the coordinates with respect to time

$$\begin{bmatrix} \dot{X} \\ \dot{Y} \end{bmatrix} = J \begin{bmatrix} \dot{\theta}_1 \\ \dot{\theta}_2 \end{bmatrix} \quad (13)$$

Here [J] is Jacobian, [J] =
$$\begin{bmatrix} \frac{\partial X}{\partial \theta_1} & \frac{\partial X}{\partial \theta_2} \\ \frac{\partial Y}{\partial \theta_1} & \frac{\partial Y}{\partial \theta_2} \end{bmatrix} \quad (14)$$

$$X = C_1L_1 + L_2C_{12} \quad (15)$$

$$\frac{\partial X}{\partial t} = \frac{\partial(C_1L_1 + L_2C_{12})}{\partial \theta_1} \frac{\partial \theta_1}{\partial t} + \frac{\partial(C_1L_1 + L_2C_{12})}{\partial \theta_2} \frac{\partial \theta_2}{\partial t} \quad (16)$$

$$\dot{X} = (-S_1L_1 - L_2S_{12}) \dot{\theta}_1 - L_2S_{12} \dot{\theta}_2 \quad (17)$$

$$Y = S_1L_1 + L_2S_{12} \quad (18)$$

$$\frac{\partial Y}{\partial t} = \frac{\partial(S_1L_1 + L_2S_{12})}{\partial \theta_1} \frac{\partial \theta_1}{\partial t} + \frac{\partial(S_1L_1 + L_2S_{12})}{\partial \theta_2} \frac{\partial \theta_2}{\partial t} \quad (19)$$

$$\dot{Y} = (C_1L_1 + L_2C_{12}) \dot{\theta}_1 + L_2C_{12} \dot{\theta}_2 \quad (20)$$

$$\begin{bmatrix} \dot{X} \\ \dot{Y} \end{bmatrix} = \begin{bmatrix} -S_1 L_1 - L_2 S_{12} & -L_2 S_{12} \\ C_1 L_1 + L_2 C_{12} & L_2 C_{12} \end{bmatrix} \begin{bmatrix} \dot{\theta}_1 \\ \dot{\theta}_2 \end{bmatrix} \quad (21)$$

$$\begin{bmatrix} \dot{X} \\ \dot{Y} \end{bmatrix} = [J] \begin{bmatrix} \dot{\theta}_1 \\ \dot{\theta}_2 \end{bmatrix} \quad (22)$$

$$\begin{bmatrix} \dot{\theta}_1 \\ \dot{\theta}_2 \end{bmatrix} = J^{-1} \begin{bmatrix} \dot{X} \\ \dot{Y} \end{bmatrix} \quad (23)$$

2.4. Dynamics

The arm dynamics of Robot handles with the mathematical formulation of the equations of robot arm motion. One methodology, named Newton-Euler Approach, is employed to derive the equations of motion. The following are final equations for joint torques [16]

$$\tau_1 = M_{11}\ddot{\theta}_1 + M_{12}\ddot{\theta}_2 + C_1 \quad (23)$$

$$\tau_2 = M_{21}\ddot{\theta}_1 + M_{22}\ddot{\theta}_2 + C_2 \quad (24)$$

Where $M_{11} = Z_1 + 2Z_2 \cos \theta_2$ (25)

$$M_{12} = M_{21} = Z_3 + Z_2 \cos \theta_2 \quad (26)$$

$$M_{22} = Z_3 \quad (27)$$

$$C_1 = -Z_2 \sin \theta_2 (\dot{\theta}_2^2 + 2\dot{\theta}_1 \dot{\theta}_2) \quad (28)$$

$$C_2 = Z_2 \dot{\theta}_1 \sin \theta_2 \quad (29)$$

$$Z_1 = M_1 r_1^2 + M_2 (L_1^2 + r_2^2) + I_1 + I_2 \quad (30)$$

$$Z_2 = M_2 L_1 r_1 \quad (31)$$

$$Z_3 = M_2 r_2^2 + I_2 \quad (32)$$

Here, r_1 and r_2 are the mass centres of links 1 and 2. I_1 and I_2 are mass moments of inertia of links 1 and 2. It is clear that mass matrix is function of joint angles and Coriolis vector components C_1 and C_2 are functions of joint angles and their time derivatives.

2.5. Solution of Dynamic Equations

Above dynamic equations are used for finding torques it is called inverse dynamics. If torques are given and thetas are required, it is called forward dynamics. Forward dynamics solution can be obtained by solving simultaneously two second order differential equations. Generally numerical methods can be used for solving these equations. One of such technique is called Runge-Kutta fourth order method. It is described for solving the equation $y' = f(x)$ as follows

$$k_1 = hf(x_0, y_0) \quad (33)$$

$$k_2 = hf\left(x_0 + \frac{1}{2}h, y_0 + \frac{1}{2}k_1\right) \quad (34)$$

$$k_3 = hf\left(x_0 + \frac{1}{2}h, y_0 + \frac{1}{2}k_2\right) \quad (35)$$

$$k_4 = hf(x_0 + h, y_0 + k_3) \quad (36)$$

$$y_1 = y_0 + \frac{1}{6}(k_1 + 2k_2 + 2k_3 + k_4) \quad (37)$$

Here $y_0 = f(x_0)$ is initial condition.

2.6. Computed torque control method (CTC)

The architecture of a non linear model based controlling mechanism called the computed torque control. A model based controller is dependent on the model of the system to be controlled. CTC is well known model based controllers that relies on calculation of system dynamics matrices iteratively at each controlling step. The matrices M, C, G of the model are recalculated at every iteration. This is due to the fact that the dynamics of a variant system is constantly subject to change. As a result, a problem that becomes more severe for complex systems. The CTC is also respected as a feed-back linearization controller in that it tries to neutralize the effects of system dynamics in the feed-back loop by cancelling the dynamic terms.

Chapter 3

Results and Discussions

3.1. Workspace Analysis

The determination of the workspaces is very useful in the context of design or motion planning of manipulators. Fig.3 shows the maximum workspace is obtained by varying the joint angles as follows: $\theta_1 \in [-170, 170]$ and $\theta_2 \in [-160, 160]$.

For finding the workspace a C program is used. Table.3.1 shows the manipulator geometric parameters considered in the present work for both kinematics and dynamic calculations.

Table 2: Two-link arm geometric parameters

S.No	Parameter	Length (m)	Mass (kg)	Moment of Inertia (kg-m ²)
1	Link-1	0.15	0.1	1.33×10^{-5}
2	Link-2	0.15	0.1	1.33×10^{-5}



Fig.4 Workspace

3.2. Manipulability Index of the manipulator

Manipulability provides quantitative measure of closeness of manipulator to singularity. Arrangement of joint parameters properly minimizes incidence of singularities. It is mathematically defined as

$$\text{Manipulability} = \sqrt{\det(J(q)J^T(q))} = \sigma_1\sigma_2 \quad (42)$$

Where σ_1 and σ_2 are singular values of matrix $J(q)$.

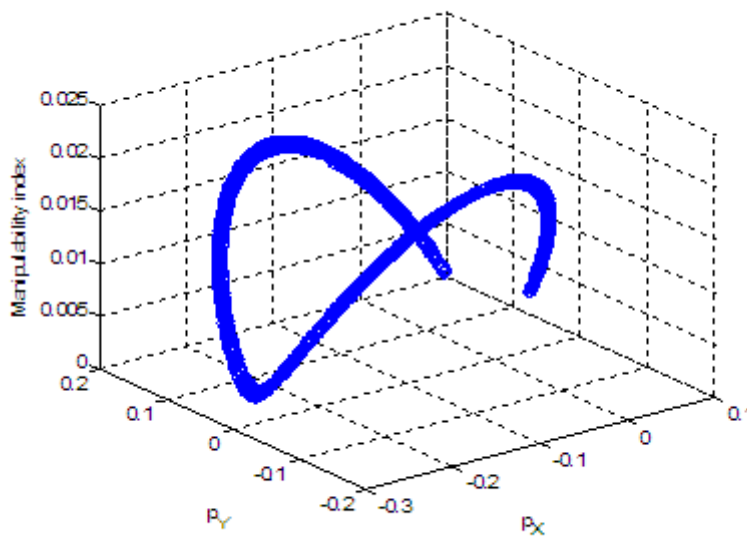


Fig.5 Manipulability index

From Fig.5 it is seen that the entire workspace is not filled but few points are only visible indicating that the singular space is much less than total workspace.

3.3. Static Force Analysis

Manipulator will produce forces and moments at the end effector in the direction of x, y and z directions. Consider $F=(F_x, F_y)^T$ denotes torques and vector of forces at the end effector. Thus the forces and torques in x, y and z directions are the components at the end effector.

$$\begin{bmatrix} \tau_1 \\ \tau_2 \end{bmatrix} = [J]^T \begin{bmatrix} F_x \\ F_y \end{bmatrix} \quad (43)$$

By selecting joint space trajectories with a constant force $F_x=10$ N and $F_y=10$ N, we can plot the joint torques. This analysis can be used for low speed applications.

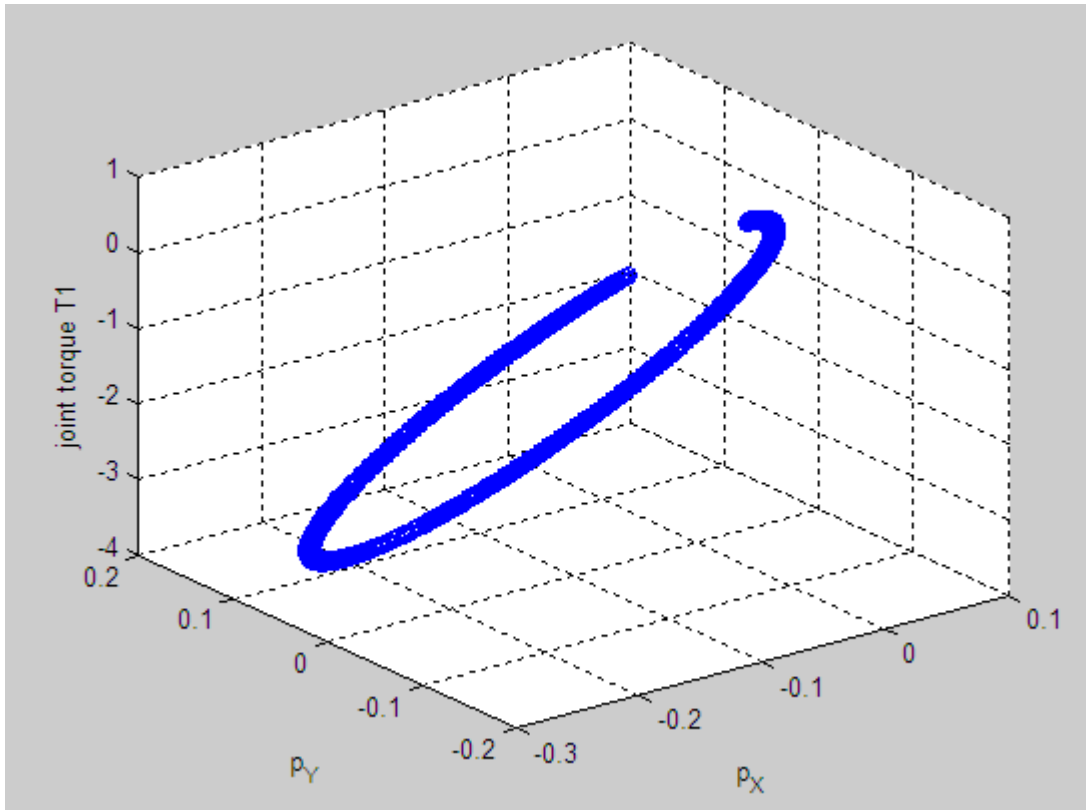


Fig.6 Joint torque T_1

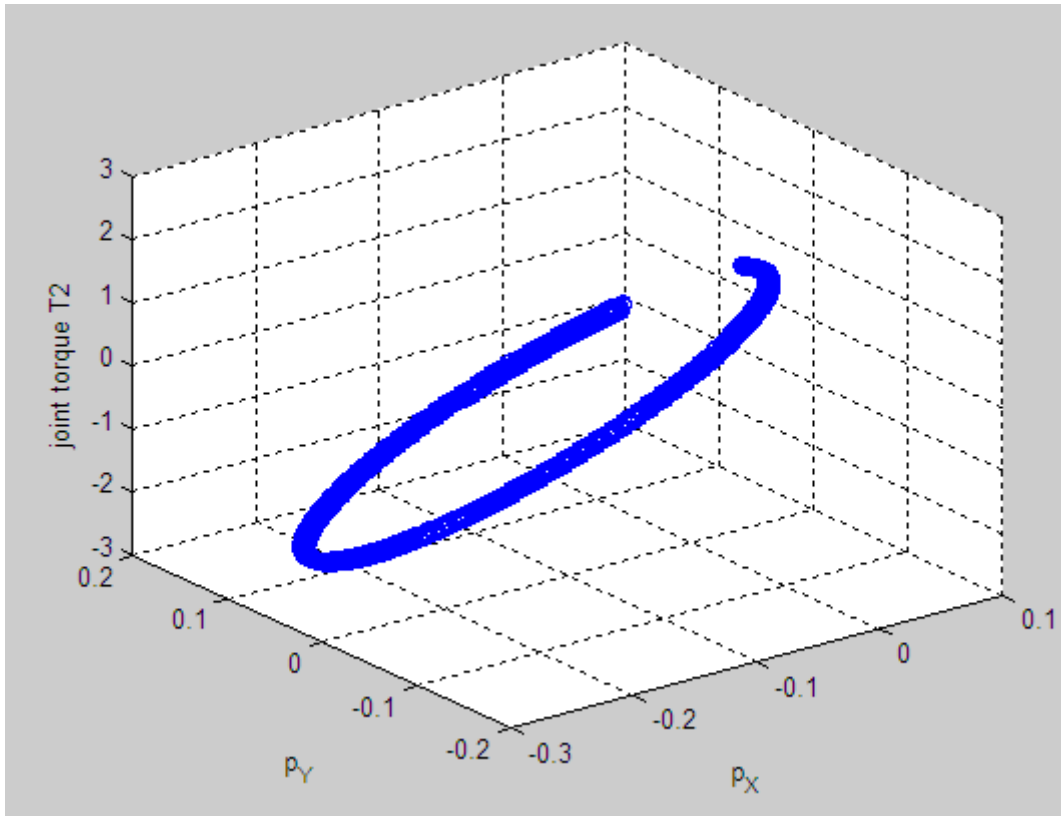


Fig.7 Joint torque T_2

3.4. Inverse dynamics analysis

Inverse dynamic analysis has been done for the joint space spiral trajectory considered for the controller design. Fig.8 illustrate the driving torques (τ_1, τ_2) of the two link manipulator from the knowledge of the trajectory equation in terms of time.

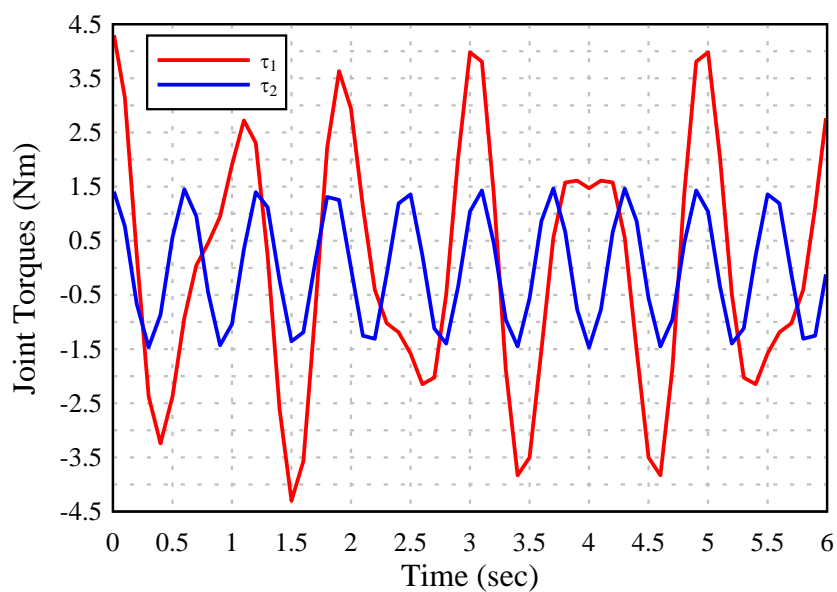


Fig.8 Joint torques

3.5 Results of Inverse kinematics

Inverse kinematic analysis results are obtained from another simple computer program. Here the end coordinates (P_x, P_y) are provided as inputs and two set of solutions for joint angles are obtained as outputs.

Table 3: Inverse kinematics solutions

(P_x, P_y) (cm)	θ_1, θ_2 (degrees)	θ_1, θ_2 (degrees)
(5, 15)	29, 76	114, 76
(13,13)	19, 34	71, -47
(10,10)	-6, 90	96,-90
(10,15)	5,51	62,-51

3.6 Control Results

The simulation results of the computed torque controller (CTC) for a two link robotic arm are presented. The program was written in C language (see appendix 2). Simulation results prove that the performance of the conventional CTC is good and the obtained figures illustrate that the tracking abilities of trajectories considered.

Trajectory 1: Straight line

A straight line trajectory is tracked in XY plane. The trajectory is defined in joint space directly as follows:

Straight line Trajectory:

$$q_1 = \left(1 - \frac{t}{T}\right) \frac{2\pi}{3} + \left(\frac{t}{T}\right) \frac{\pi}{3}$$

$$q_2 = \left(1 - \frac{t}{T}\right) \left(q_1 - \frac{\pi}{3}\right)$$

Where $t \in [0, 6.1]$ sec is time, $(x_p, y_p)^T = (2.2, -0.4)^T$ is the initial point. In simulations, the control gains are selected as follows:

$$K_p = \begin{bmatrix} 100 & 0 \\ 0 & 100 \end{bmatrix} \quad K_v = \begin{bmatrix} 20 & 0 \\ 0 & 20 \end{bmatrix}$$

Fig.10 shows the desired trajectory considered in a 3-Dimensional space.

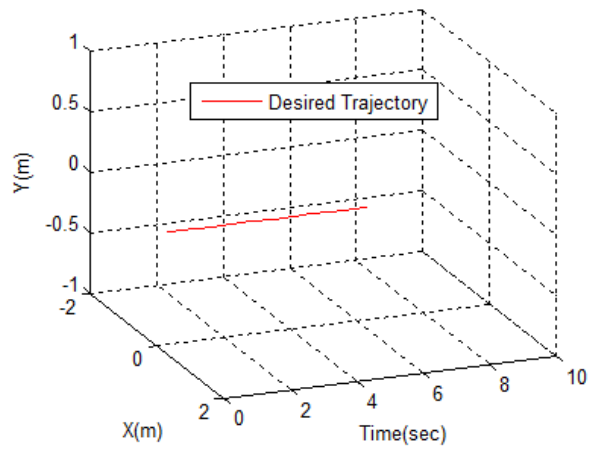


Fig.9 Desired Trajectory

Fig.11 shows the final result of the trajectory from CTC.

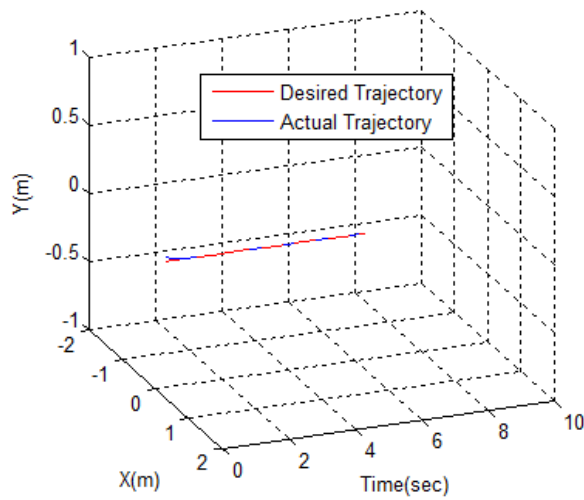


Fig.10 Trajectory tracking of the end-effector

Fig.11 shows the joint angles in every time second.

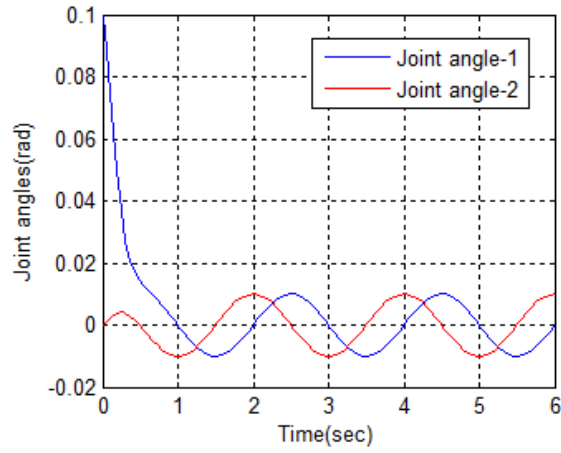


Fig.11 Joint Angles

Fig.12 shows the corresponding joint velocities

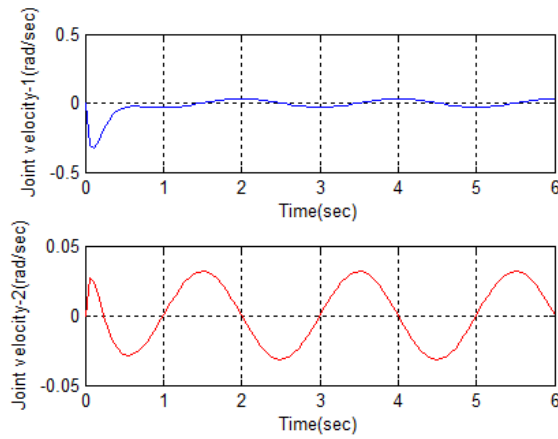


Fig.12 Joint velocities

Fig.13 shows the calculated joint torques

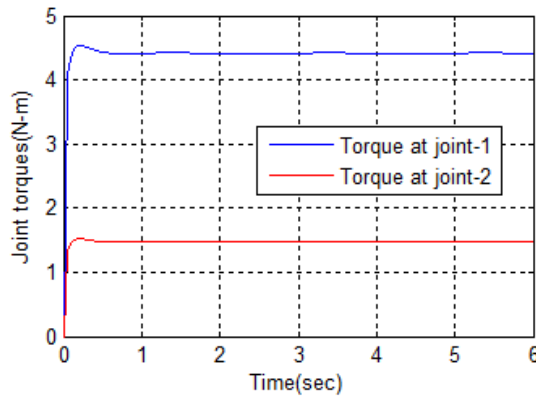


Fig.13 Control Torques

Fig. 14 shows the tracking errors at the joints of the manipulator and it is found the percentage error is less than one.

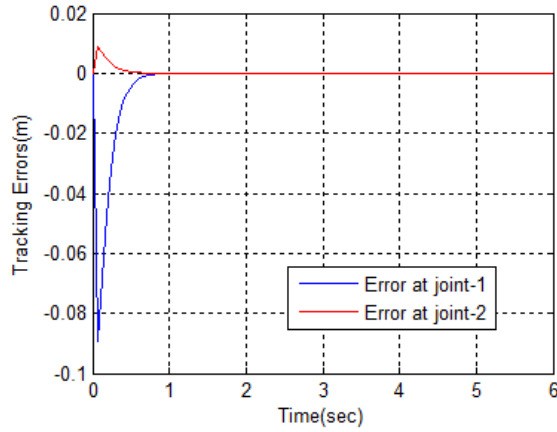


Fig.14 Tracking Errors

Trajectory 2: Spiral

A spiral trajectory is tracked in XY plane. The trajectory is defined as follows:

Spiral Trajectory:

$$\begin{cases} q_1 = (\pi/5) \times (t/T - (1/(2 \times \pi)) \times \sin(2 \times \pi \times t / \pi)) \\ q_2 = (\pi/8) \times (t/T - (1/(2 \times \pi)) \times \cos(2 \times \pi \times t / \pi)) \end{cases}$$

Where $t \in [0.1, 0.6]$ is time, $T=0.1$ is the parameter, in simulations, the control gains are selected as follows:

The parameters of the conventional CTC are set to be:

$$K_p = \begin{bmatrix} 100 & 0 \\ 0 & 100 \end{bmatrix} \quad K_v = \begin{bmatrix} 20 & 0 \\ 0 & 20 \end{bmatrix}$$

Fig.15 and 16 show the desired and actual trajectories.

Fig.17 shows control torques computed by the algorithm

Fig.18 shows the error histories. It is seen that CTC effectiveness is very good after some time has elapsed.

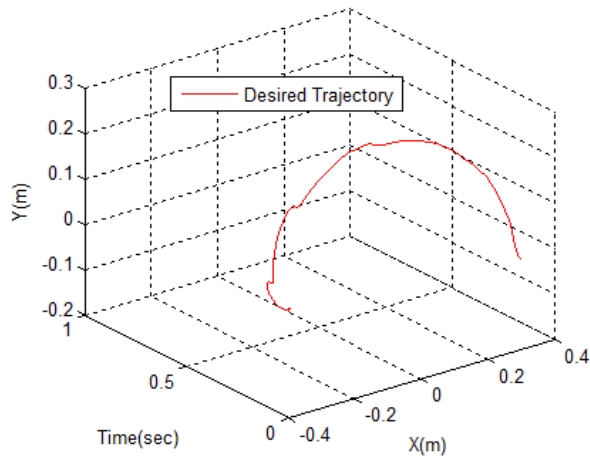


Fig.15 Desired Trajectory

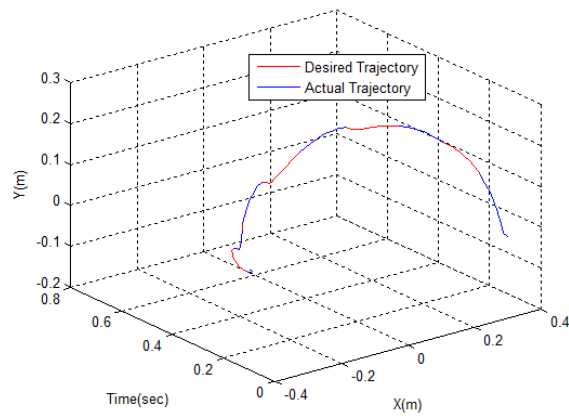


Fig.16 Trajectory Tracking of end effector

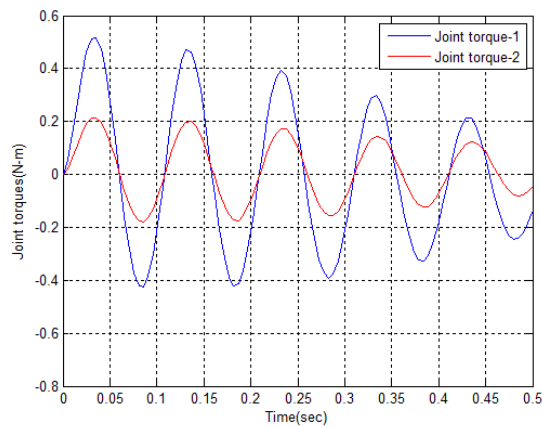


Fig.17 Control torques

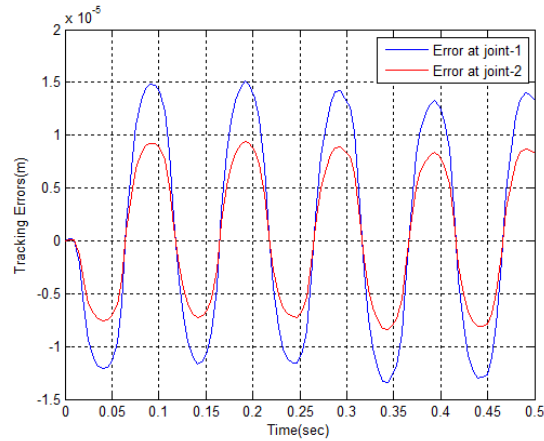


Fig.18 Tracking errors

3.6 Model Fabrication and experimental testing

In fabrication work, two links are constructed by using Aluminium sheet of finite thickness (3mm). The length of first link called L_1 is 9 cm, and second link called L_2 is 11cm. These are measured from joint to joint. L_1 is connected to the base part of system with servo motor, L_2 link is connected to L_1 through another servo motor. Two standard economy servo motors 4.5kgcm with plastic gears is used to revolute the links. Arduino Uno R3 is used to control the servos with an arduino program. The end of second link is joined with pencil for tracing in XY plane. This is revolving fully in a horizontal plane. Fig.19 shows the fabricated set-up.



Fig.19 Prototype model

Fig. 20 shows the control system based on laptop with an arduino board based on inverse kinematics

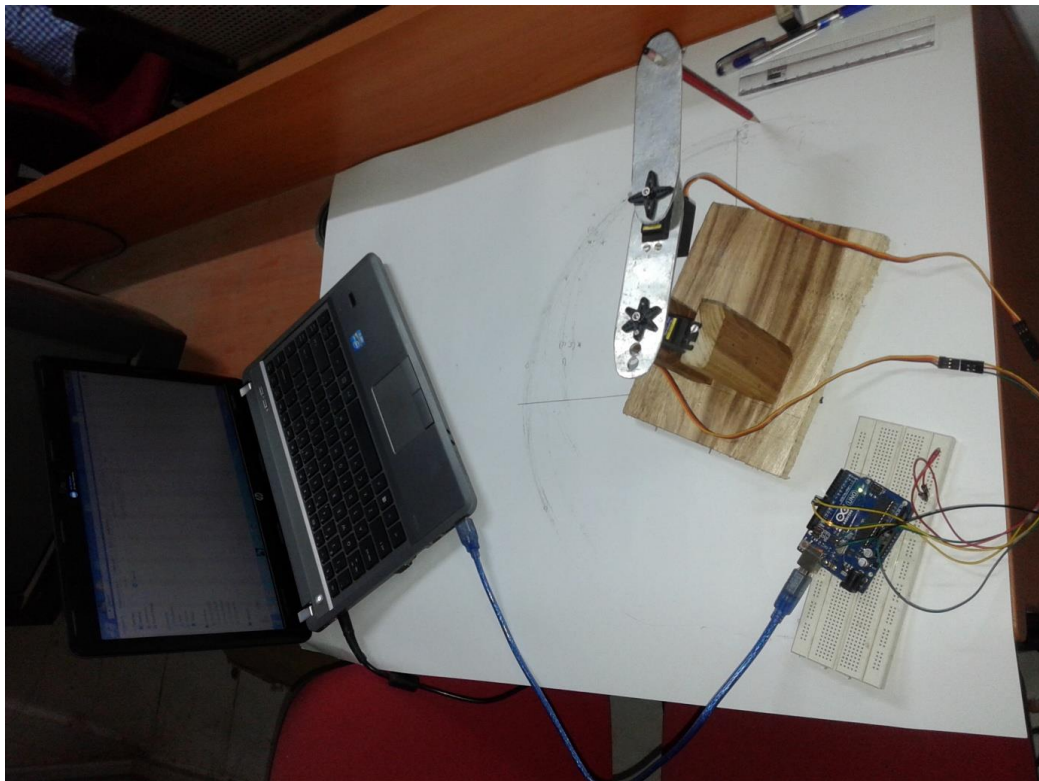


Fig.20 Control experiment for tracking the points

The points are traced by giving the joint angles θ_1 and θ_2 to the arduino microcontroller, which are obtained by the inverse kinematic equations and are shown in Table.2. The corresponding code written in arduino compiler is shown below.

```
=====
#include<servo.h>
servo servo 1; // define left servo
servo servo 2; // define right servo

void setup(){
servo 1.attach(10); // set left servo to digital pin 10
servo2.attach(9); // set right servo to digital pin 9
}

void loop() { // loop through motion test
p0();
delay(2000);
p1(); // example : move forward
delay(2000); // wait 2000 milliseconds
p2();
delay(2000);
}
// motion routine for forward, reverse, turns, step
void p0() {
```

```

servo1.write(0);
servo2.write(0);
}

void p1(){
servo.write(0);
servo2.write(180);
}

void p2(){
servo1.write(180);
servo2.write(0);
}

```

Initial position of the end effector is (20, 0) (along horizontal axis) where the location of both the servo motors angular position are 0 degrees.

Table 4: Trajectory tracking for inverse kinematics

(P _x , P _y) (cm)	θ ₁ , θ ₂ (degrees)	θ ₁ , θ ₂ (degrees)
(5, 15)	29, 76	114, 76
(13,13)	19, 34	71, -47

Fig. 21 shows the trajectory traced by the end effector pencil tool with respect to original points. It is seen that at every point some error is occurring. This may be due to inaccuracies in the model setting including the pencil tool alignment as well as due to the integer values of joint angles given to the arduino program.

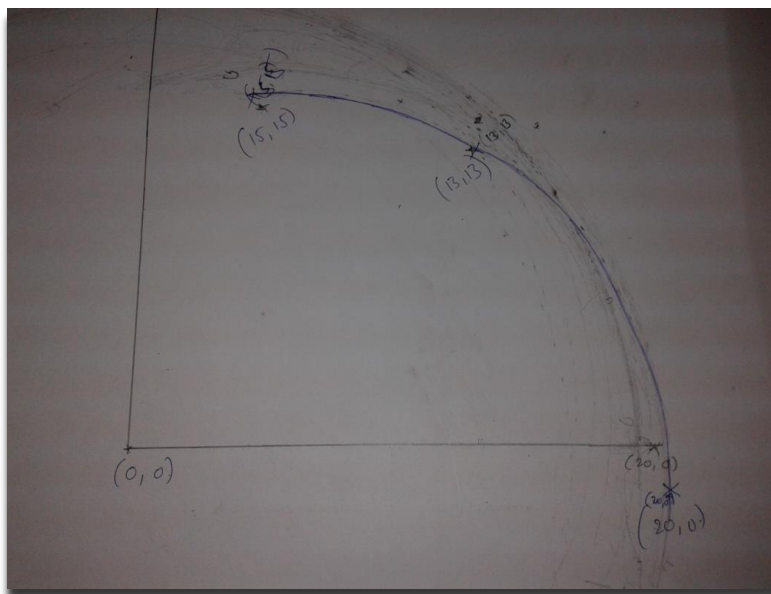


Fig.21 Experimental plot for inverse kinematics

Chapter 4

CONCLUSION

In this work several aspects regarding the kinematics, workspace, Jacobian analysis and dynamic identification of a two-link planar manipulator were presented. The results obtained in this study may be useful for the robot designing not only to understand the kinematic behaviour of the robot for various configurations, but also to be able to implement real time control of a manipulator. The programs are developed in C language for generation of workspace points, manipulability index based on Jacobian and for inverse kinematics. The results obtained are plotted separately from data files. Even though the two link manipulator is relatively simple and straight forward, most of the approaches applied here are common to all the manipulators. The static force analysis for obtaining joint torques is a important problem for design of manipulator. Finally the trajectory tracking problem with two different trajectories using CTC control method was illustrated numerically. The errors and corresponding applied torques were shown as a function of time. This two link manipulator analysis and control is an on going work in mechatronics and robotics research.

4.1. Future scope

The CTC control can be improved by tuning of position and velocity gain constants. Also, when a disturbance such as a payload at the gripper acts on the system, the CTC algorithm requires slight modification by adding additional control torque obtained from disturbance rejection observer. This can be added to present work as a future scope. The scaled model developed can be improved further to perform pick and place operations by attaching a two finger gripper. This can be extended to a redundant four degree of freedom, spatial SCARA manipulator with one translational joint. During the control, the manipulator joint torques (hence angles) are to be computed automatically while tracking the trajectory is going on. An improvised experimental work is required.

References

- 1) A. De Luca and B. Siciliano. Closed-Form Dynamic Model of Planar Multilink Lightweight Robots. *IEEE Trans. Syst., Man, Cybern.* 1991; vol. 21, no. 4; pp. 826- 839.
- 2) A. W. William, *Automatic Control Systems Basic Analysis and Design*, Oxford University Press, 1995; pp. 219-223.
- 3) Y. Kwanho. *Adaptive Control*, In-Tech publication, 2009; pp. 87-112.
- 4) I. J. Nagrath and M. Gopal, *Control Systems Engineering*, New Age Publisher, 2007.
- 5) M. O. Tokhi and A.K.M. Azad, *Flexible Robot Manipulators Modeling, Simulation and Control*, IET, London, UK, 2008.
- 6) A. A. Ata. Optimal Trajectory Planning Of Manipulators: A review. *J Engg. Sci. Tech.* 2006; pp. 32–54.
- 7) S. Islam and X. P. Liu. Robust Sliding Mode Control for Robot Manipulators. *IEEE Trans. Ind. Elect.* 2011; vol. 58; pp. 2444–2453.
- 8) N. Kumara, V. Panwarb and N. Sukavanamc. Neural Network-Based Nonlinear Tracking Control of Kinematically Redundant Robot Manipulators. *Math. Comp. Modelling.* 2011; vol. 53; pp.1889–1901.
- 9) F. Moldoveanu, V. Comnac and D. Floroia. Trajectory Tracking Control of a Two-Link Robot Manipulator using Variable Structure System Theory. *Control Engg. App. Info.* 2005; vol. 7; pp. 56–62.
- 10) A. Wang and M. Deng. Robust Nonlinear Control Design to a Manipulator Based on Operator based Approach. *ICIC Express Letters* 2012; vol. 6; pp.617–623.
- 11) Y. Zhu, J. Qiu and J. Tani. Simultaneous Optimization of a Two-Link Flexible Robot Arm. *J. Robo. Syst.* 2011; vol. 18; pp. 29–38.
- 12) F. Ionescu. Modeling and Simulation in Mechatronics. *IFAS Int. Conf, MCPL* 2007; pp.26-29.
- 13) H. Karagulle and L. Malgaca, Analysis For End Point Vibrations Of Two Link Manipulator By Integrated CAD/CAE Procedures. *Finite Elem. Ana. Design.* 2004; vol. 40; pp. 2049-2061.
- 14) S. P. Nagesh Rao, G. Lopes, D. Jeltsema and R. Babuska. Passivity Based Reinforcement Learning Control of a 2-DOF Manipulator Arm. *Mechatronics.* 2014; vol. 24; pp.1001-1007.
- 15) H. V. H. Ayala, L. D. S. Coelho. Tuning of PID Controller Applied to a Robotic Manipulator. *Exp. Syst. App.* 2012; vol. 39; pp. 8968-8974.
- 16) A. Wang and M. Deng, Robust non linear multi variable tracking control design to a manipulator with unknown uncertainties using operator based robust right coprime factorization, *Transactions of institute of measurement and control*, DOI 10.1177/0142331212470838, 2013.

Appendix 1

WORKSPACE AND KINEMATICS PROGRAM

C Program for workspace, Jacobian, manipulability index, static force analysis.

```
#include<stdio.h>
#include<math.h>
main()
{
int i;
double a1,a2,th1,th2,pi,px,py,Th1,Th2,Px,Py,invkin;
double B1,B2,B3,B4,J11,J12,J21,J22,Mani,tou1,tou2,F1,F2;
FILE *fp;
fp=fopen("wspace.c","w");
a1=0.15;
a2=0.15;
pi=22.0/7.0;
F1=10;
F2=10;
//i=1;
clrscr();
for(th1=-170;th1<170;th1=th1+5)
{
for(th2=-160;th2<160;th2=th2+5)
{
Th1=th1*pi/180.0;
Th2=th2*pi/180.0;
px=a1*cos(Th1)+a2*cos(Th1+Th2);
py=a1*sin(Th1)+a2*sin(Th1+Th2);
J11=-a1*sin(Th1)-a2*sin(Th1+Th2);
J12=-a2*sin(Th1+Th2);
J21=a1*cos(Th1)+a2*cos(Th1+Th2);
J22=a2*cos(Th1+Th2);
B1=J11*J11+J21*J21;
B2=J12*J12+J21*J22;
B3=J12*J11+J22*J21;
B4=J12*J12+J22*J22;
Mani=sqrt(B1*B4-B2*B3);
tou1=J11*F1+J21*F2;
tou2=J12*F1+J22*F2;
i=i+1;
fprintf(fp,"%f\t%f\t%f\t%f\t%f\t%f\t%f\t%f\n",th1,th2,px,py,Mani,tou1,tou2);
}
}
}
//Px=0.3;
//Py=0.1;
//invkin(Px,Py);
//printf("i=%d\n",i);
//getch();
/*double invkin(double px,double py);
{
double c2n,c2d,c2,s2,c1n,c1d,c1,s1,a1,a2,TH1,TH2;
FILE *fp;
c2n=(px*px+py*py-a1*a1-a2*a2);
c2d=2*a1*a2;
c2=c2n/c2d;
s2=sqrt(1-c2*c2);
TH2=atan2(s2,c2);
c1n=(px*(a1+a2*cos(TH2)))+(py*a2*sin(TH2));
c1d=(px*px+py*py);
c1=c1n/c1d;
s1=sqrt(1-c1*c1);
TH1=atan2(s1,c1);
fprintf(fp,"%f\t%f\t%f\t%f\t%f\n",TH1,TH2,px,py);
getch();}
```

Appendix 2

CTC PROGRAM IN 'C' LANGUAGE

C Programming code for CTC control.

```

#include<stdio.h>
#include<math.h>
#define m1 0.1
#define m2 0.1
#define a1 0.15
#define a2 0.15
#define Z1
#define Z2
#define Z3
main()
{
int i;
double kp1,kd1,kp2,kd2,px,py,px0,py0,pxd,pyd,pxdd,pydd,t,r,pi,X,Xa,Xd,c2n,c2d,c2,s2;
double thd,th1,th2,c1n,cld,c1,s1,J[2][2],JT[2][2],JI[2][2],e[2][1],ed[2][1];
double a1,a2,F1,F2;
FILE *fp;
fp=fopen("dynamic.c","w");
px0=0.3;
py0=0.3;
r=0.01;
pi=22.0/7.0;
i=0;
//desired trajectory
for(t=0;t<2*pi;t=t+0.01)
{
px=px0+r*cos(t);
py=py0+r*sin(t);
pxd=-r*sin(t);
pyd=r*cos(t);
pxdd=-r*cos(t);
pydd=-r*sin(t);
//Inverse kinematics
c2=(px*px+py*py-a1*a1-a2*a2)/(2*a1*a2);
s2=sqrt(1-c2*c2);
th2=atan2(s2,c2);
s1=((a1+a2*c2)*py-px*a2*s2)/(a1*a1+a2*a2+2*a1*a2*c2);
c1=(px+s1*a2*s2)/(a1+a2*c2);
th1=atan2(s1,c1);
// JACOBIAN
J[0][0]=-s1*a1-a2*sin(th1+th2);
J[0][1]=-a2*sin(th1+th2);
J[1][0]=c1*a1+a2*cos(th1+th2);
J[1][1]=a2*cos(th1+th2);
detJ=J[0][0]*J[1][1]-J[0][1]*J[1][0];
JI[0][0]=J[0][0]/detJ;JI[0][1]=-J[1][0]/detJ;
JI[1][0]=-J[0][1]/detJ;JI[1][1]=J[1][1]/detJ;
th1d=JI[0][0]*pxd+JI[0][1]*pyd;
th2d=JI[1][0]*pxd+JI[1][1]*pyd;
if(i==0)
{
F1=rand();
F2=rand();
}
else
{
//compute errors
eth1=th1-th1a;
eth2=th2-th2a;
eth1d=th1d-th1da;

```

```

eth2d=th2d-th2da;
//pd control gains
kp1=100;
kd1=20;
kp2=100;
kd2=200;
b1=th1dd+kp1*eth1+kd1*eth1d;
b2=th2dd+kp2*eth2+kd2*eth2d;
Z1=m1*r1*r1+m2*(a1*a1+r2*r2)+I1+I2;
Z2=m2*a1*r1;
Z3=m2*r2*r2+I2;
M11=Z1+2*Z2*cos(th2);
M12=Z3+Z2*cos(th2);
M21=M12;
M22=Z3;
C1=-Z2*sin(th2)*(th2d*th2d+2*th1d*th2d);
C2=Z2*th1d*th1d*sin(th2);
//Compute control torques
F1=M11*b1+M12*b2+C1;
F2=M21*b1+M22*b2+C2;
}
[th1a,th1ad,th2a,th2ad]=dynam(F1,F2,th1,th2,thd1,thd2);
Tor1[i1]=F1;Tor2[i1]=F2;
e1[i1]=eth1;e2[i1]=eth2;
fprintf(fp,'%f\t%f\t%f\t%f\t%f\n',t,F1,F2,eth1,eth2);
i1=i1+1;
}
}

dynam(double F1,double F2,double th1,double th2,double thd1,double thd2)
{
double f1,g1,j1,k1;
double f2,g2,j2,k2,f3,g3,j3,k3,f4,g4,j4,k4;
double f(),g(),j(),k(),x1,x2,x3,x4;
//Compute inertia matrix
//Z1=m1*ag1*ag1+m2*(a1*a1+ag2*ag2)+I1+I2;//Z2=m2*a1*ag2;//Z3=m2*ag2*ag2+I2;
//m11=Z1+2*Z2*cos(th2);
//m12=Z3+Z2*cos(th2);
//m21=m12;
//m22=Z3;
x1=th1;x2=th1d;x3=th2;x4=th2d;
for (i2=0;i2<200;i2++)
{
f1=h*f(t,x1,x2,x3,x4); g1=h*g(t,x1,x2,x3,x4);
j1=h*j(t,x1,x2,x3,x4); k1=h*k(t,x1,x2,x3,x4);
f2=h*f((t+h/2),(x1+f1/2),(x2+g1/2),(x3+j1/2),(x4+k1/2));
g2=h*g((t+h/2),(x1+f1/2),(x2+g1/2),(x3+j1/2),(x4+k1/2),F1,F2);
j2=h*j((t+h/2),(x1+f1/2),(x2+g1/2),(x3+j1/2),(x4+k1/2));
k2=h*k((t+h/2),(x1+f1/2),(x2+g1/2),(x3+j1/2),(x4+k1/2),F1,F2);
f3=h*f((t+h/2),(x1+f2/2),(x2+g2/2),(x3+j2/2),(x4+k2/2));
g3=h*g((t+h/2),(x1+f2/2),(x2+g2/2),(x3+j2/2),(x4+k2/2),F1,F2);
j3=h*j((t+h/2),(x1+f2/2),(x2+g2/2),(x3+j2/2),(x4+k2/2));
k3=h*k((t+h/2),(x1+f2/2),(x2+g2/2),(x3+j2/2),(x4+k2/2),F1,F2);
f4=h*f((t+h),(x1+f3),(x2+g3),(x3+j3),(x4+k3));
g4=h*g((t+h),(x1+f3),(x2+g3),(x3+j3),(x4+k3),F1,F2);
j4=h*j((t+h),(x1+f3),(x2+g3),(x3+j3),(x4+k3));
k4=h*k((t+h),(x1+f3),(x2+g3),(x3+j3),(x4+k3),F1,F2);
x1=x1+((f1+f4)+2*(f2+f3))/6.0;
x2=x2+((g1+g4)+2*(g2+g3))/6.0;
x3=x3+((j1+j4)+2*(j2+j3))/6.0;
x4=x4+((k1+k4)+2*(k2+k3))/6.0;
}
return();
}
double f(double t1,double q1,double q1d,double q2,double q2d)
{

```

```

return(q1d);
}
double g(double t1,double q1,double q1d,double q2,double q2d,double F1,double F2)
{
double m11,m12,m21,m22,c1,c2;
m11=Z1+2*Z2*cos(q2);
m12=Z3+Z2*cos(q2);
m21=m12;
m22=Z3;
//Compute corialisis matrix
c1=-Z2*sin(q2)*(q2d*q2d+2*q1d*q2d);
c2=Z2*q1d*q1d*sin(q2);
return((F1*m22-c1*m22-m12*F2+c2*m12)/(m11*m22-m12*m12));
}
double j(double t1,double q1,double q1d,double q2,double q2d)
{
return(q2d);
}
double k(double t1,double q1,double q1d,double q2,double q2d,double F1,double F2)
{
double m11,m12,m21,m22,c1,c2;
m11=Z1+2*Z2*cos(q2);
m12=Z3+Z2*cos(q2);
m21=m12;
m22=Z3;
//Compute corialisis matrix
c1=-Z2*sin(q2)*(q2d*q2d+2*q1d*q2d);
c2=Z2*q1d*q1d*sin(q2);
return((F1*m12-c1*m12-m11*F2+c2*m11)/(m12*m12-m11*m22));
}

```